Neuroprotective Effects of Oxymatrine via Triggering Autophagy and Inhibiting Apoptosis Following Spinal Cord Injury in Rats

Jian Li
First Affiliated Hospital of Jinzhou Medical University
Yang Cao
First Affiliated Hospital of Jinzhou Medical University
Lin-Na Li
First Affiliated Hospital of Jinzhou Medical University
Xin Chu
First Affiliated Hospital of Jinzhou Medical University
Yan-Song Wang
First Affiliated Hospital of Jinzhou Medical University
Jia-Jun Cai
First Affiliated Hospital of Jinzhou Medical University
Jin Zhao
First Affiliated Hospital of Jinzhou Medical University
Song Ma
First Affiliated Hospital of Jinzhou Medical University
Gang Li
Shandong University Cheeloo College of Medicine
Zhongkai Fan (fanzk_ln@163.com)
First Affiliated Hospital of Jinzhou Medical University https://orcid.org/0000-0002-3448-9698

Research Article

Keywords: Autophagy, Apoptosis, Spinal cord injury (SCI), Oxymatrine, SIRT1, AMPK

Posted Date: April 26th, 2022

DOI: https://doi.org/10.21203/rs.3.rs-1553538/v1

Version of Record: A version of this preprint was published at Molecular Neurobiology on April 28th, 2023. See the published version at https://doi.org/10.1007/s12035-023-03364-1.

Abstract

The identification of drugs that promote autophagy and inhibits apoptosis in neurons is critical for improving patient outcomes following spinal cord injury (SCI). Here, we aimed to investigate the neuroprotective effects of oxymatrine (OMT) and the potential mechanism after SCI in rats. Female Sprague-Dawley rats were randomly assigned to either a sham group, SCI group, OMT-treated group (40 mg/kg), and a group treated with both OMT and SIRT1 inhibitor EX527 (10 μg/kg). A modified compressive device (weight 35 g, time 5 min) was applied to induce moderate SCI in all groups except the sham group. After treatment with drugs or vehicle (saline), the neurological functions were evaluated using the Basso, Beattie, and Bresnahan (BBB) locomotor rating scale and footprint analysis. Morphological changes in the spinal cord were assessed using hematoxylin-eosin staining and the number of surviving and apoptotic neurons was determined using Nissl and TUNEL staining, respectively. Neuronal ultrastructures were observed using transmission electron microscope (TEM). Moreover, we investigated the gene and protein expression levels of relevant molecules involved in apoptosis and autophagy, such as SIRT1, AMPK, p62, Beclin-1, LC3B, Bcl-2, Bcl-xL, Bax, Bak and C-caspase-3 using qRT-PCR analysis, Western blotting, or immunofluorescence staining. Our results indicated that OMT treatment significantly reduced the lesion size, promoted survival of motor neurons, and subsequently attenuated motor dysfunction following SCI in rats. OMT significantly enhanced autophagy activity, inhibited apoptosis in neurons, and increased SIRT1 and p-AMPK expression levels. These effects of OMT on SCI were partially prevented by co-treatment with SIRT1 inhibitor EX527. Taken together, these data revealed that OMT exerts a neuroprotective role in functional recovery against SCI in rats, and these effects are potentially associated with OMT-induced activation of autophagy via the SIRT1/AMPK signaling pathway.

Introduction

Spinal cord injury (SCI) is a catastrophic central nervous system (CNS) disorder consisting mainly of two pathological phases, primary injury [1] and secondary injury [2]. The former is attributed to direct mechanical damage to the spinal cord and is irreversible, while the latter is elicited by a complicated cascade of biochemical changes following the primary injury involving edema [3, 4], autophagy [5, 6], apoptosis [7, 8], inflammation [9, 10], oxidative stress [11, 12], and scar formation [4, 13]. Importantly, secondary injury is considered to be reversible and is thought to have an even more pronounced impact on the pathogenesis of SCI than the primary injury [11, 14]. To date, there are several potential treatments of SCI involves gene, molecule and drugs therapy, however, only methylprednisolone (MP) has demonstrated efficacy in clinical trials and thus has been used commonly in the treatment of patients with SCI [15]. In recent years, a series of complications induced by high-dose protocol of MP has been gradually emerging such as pneumonia, sepsis, wound infections, gastrointestinal bleeding, as well as thromboembolism, indicating MP administration after SCI carries some substantial risks [15–17]. Therefore, identifying more effective clinical drugs preventing or alleviating secondary injury is of vital importance.

Neuronal apoptosis, one of the most prominent pathological features of secondary SCI, and the resultant neuronal loss can seriously impede the recovery of locomotor functions following SCI in rats [1, 5, 18]. Autophagy is the main catabolic mechanism for cells to degrade intracellular proteins and organelles in the cytoplasm by the autophagosomal–lysosomal pathway and plays a crucial role in the maintenance of cellular homeostasis and regulation of both physiological and pathological processes in the CNS [19–21]. The autophagy process is believed to closely related to apoptosis [22, 23]. Emerging data have shown that autophagy can exhibit dual role, both beneficial and detrimental, following CNS injuries, possibly depending on the location and severity of the injury [24, 25]. Nonetheless, it appears clearly that enhancing autophagic flux may significantly accelerate neurological functional recovery by inhibiting neuronal apoptosis following moderate SCI models of rats [5, 7], which suggests that modulation of the autophagy pathway could represent a promising therapeutic strategy for SCI.

Silent information regulators (SIRTs or Sirtuins) are a family of conserved nicotinamide adenine dinucleotide (NAD+)-dependent histone deacetylase, which consist of 7 mammalian members (SIRT1–7) [26]. That functions of SIRTs vary depends on their subcellular distribution. SIRT1, localized mainly in the nucleus, has been indicated to play a critical role in the regulation of several physiological and pathological processes, including metabolism, autophagy, apoptosis, inflammation, oxidative stress, and aging [27–30]. Compelling in vivo and in vitro evidence that the levels of autophagy and apoptosis are interlinked with the SIRT1/AMPK (AMP-activated protein kinase) signaling pathway [31–33]. After SCI in rats, the SIRT1 activator resveratrol has been shown to promote activation of the autophagy pathway by modulating AMPK activity [31]. Moreover, melatonin has been shown to significantly enhance autophagy and inhibit apoptosis in neurons, thereby promoting the neurological functional recovery via activation of the SIRT1/AMPK signaling pathway in a SCI rat model [32]. These previous studies suggested that the SIRT1/AMPK signaling pathway plays an essential role in the regulation of neuronal autophagy and apoptosis following SCI in rats.

Oxymatrine (OMT) (Fig. 1A), classified as a quinolizidine alkaloid, is a phytochemical product extracted from the traditional Chinese medicinal herb-*Sophora flavescens*. OMT is primarily a chemotherapeutic agent used in treatment of a wide variety of cancers [34, 35]. Due to its wide range of pharmacological properties, including anti-viral [36], anti-inflammatory [37], anti-apoptotic [38], anti-oxidative [39], and anti-immune [40] effects, OMT has successfully been used for the treatment of various diseases, such as chronic hepatitis [41], bronchial asthma [36], and several disorders involving ischemia/reperfusion injuries in the heart [42], lung [43], liver [38], kidney [39], intestine [44], and brain [45, 37]. After hippocampal ischemia-reperfusion injury in rats, OMT can mediate neuroprotection by enhancing autophagy via upregulation of SIRT1 expression and thereby attenuating injury-induced cognitive deficits [46]. Recently, Guan et al. [10] have demonstrated that OMT was able to elicit neuroprotective effects following SCI by reducing inflammation, oxidative stress, and apoptosis. However, the effects and exact molecular mechanisms of OMT on the autophagic activity of neuronal cells in the spinal cord following SCI have not been elucidated. Here, we hypothesized that OMT could promote neuronal autophagy, reduce neural tissue

damages, and ultimately alleviate locomotor impairments via activation of the SIRT1/AMPK signaling pathway following SCI in rats.

Materials And Methods

Animals and Experimental Groups

Animals: Eighty female Sprague–Dawley rats (weighing 180–220 g, aging 9-10 weeks old) were purchased and bred in the central animal house (12-h light/dark cycle with free access to food and water ad libitum) of Jinzhou Medical University (Jinzhou, China). All animal experiments were performed in compliance with the guidelines for the Institutional Animal Care and Use of Jinzhou Medical University. The procedures were approved by the Animal Ethics Committee of Jinzhou Medical University. Great efforts were made to reduce the number and suffering of the animals used in our study.

Experimental Groups: All rats were randomly and blindly allocated into Sham group (only laminectomy was performed without SCI induction); SCI group (underwent moderate compressive SCI after laminectomy); Single dose of OMT group (40 mg/kg, intraperitoneal injection immediately after SCI); OMT+EX527 group (abbreviated to EX527 group, a SIRT1 specific inhibitor, 10 μg/kg, intraperitoneal injection immediately after SCI). Vehicle (saline) were administrated intraperitoneally directly into the abdominal cavity at the same time point after SCI.

Establishment of Rat SCI Models

The rat models of SCI were established as our previous description [4,9]. Briefly, rats were anesthetized intraperitoneally (i.p.) with pentobarbital sodium (40 mg/kg). Following anesthesia, a 3 cm midline incision was conducted to expose the T9-T12 spinal cord following by compressing the spinal cord vertically with a sterile metal impounder (weight 35 g, diameter 2 mm) for 5 min to induce a moderate SCI model [4,9,47]. Signs of successful model were symbolized with visible injured spinal cord surface blood stasis, quick tail flick reflex and rapid tremor of the both lower limbs of the rats. Rats that have not been successfully modeled were excluded from experiments. After the surgery, the incision was sutured and all rats were allowed to recover on a 30 °C heating pad. Next, experimental rats received continuously injection of ceftriaxone sodium (50 mg/kg, i.p.) daily for 3 days and their bladders were massaged manually twice a day until the spontaneous urination was restored.

Drugs Administration

Oxymatrine (N1835) with a purity of more than 98% was purchased from the APExBIO (USA) and prepared at a final concentration of 40 mg/mL in normal saline. EX527 (S1541) with a purity of more than 99.78 % was purchased from Selleck (USA) and dissolved in normal saline to 0.04 M/L. All experimental reagents were standard commercially available. OMT (40 mg/kg) [10] and EX527 (10 μg/kg) [48,32] were administered intraperitoneally daily for consecutive 7 days until the animals were euthanized. Equal volume of saline was injected intraperitoneally at the same time points.

Assessment of Functional Locomotor Recovery

The Basso, Beattie and Bresnahan (BBB) locomotor rating scale [49] and footprint analysis [50] were conducted in our present study to assess locomotor function recovery of rats. Both of them were performed in a noise-free environment. Scores of all behavioral measures were done by observers blinded to the groups.

For BBB Scores All animals were tested at days 0, 1, 3, and 7, the highest score (21 scores) indicates normal motor capacity and the lowest score (0 score) indicates completely paralyzed. All rats were scored by three experimenters who were blind to the experimental protocols. The mean of three measurements was recorded and analyzed finally.

For Footprint Analysis All animals were tested at day 7, modified method was referred to several studies [50]. Briefly, preparing a manual dark box (50×4×4cm) paved with a white paper (60 cm long, 5 cm width) at the bottom to make a straight track. Subsequently, the animal's fore- and hindpaws were inked with red and black dyes, respectively. Induce the animals to walk forward straight by placing a food at the far end of box. The footprints were preserved and the digitized images were analyzed finally.

Sections Preparation

Rats were sacrificed at 7 days and anesthetized with pentobarbital sodium (40 mg/kg). Then, 0.9% ice-cold saline and 4% paraformaldehyde (PFA) in 0.1% phosphate-buffered saline (PBS, pH 7.4) were perfused transcardially, respectively. Subsequently, the T9-T12 spinal cord segments were removed and postfixed in 4% PFA for 1 day and dehydrated with 30% sucrose in 0.1% PBS over 2 nights at 4 °C. Afterwards, 1 cm-long spinal cord tissues around the epicenter lesion were dissociated and embedded in O.C.T compound (4583, SAKURA, USA) for cryosectioning. Serial 10 μm-thick frozen sections from the rostral-to-caudal direction were collected using a cryostat microtome (CM3050S, Leica, Heidelberg, Germany) for hematoxylin and eosin (HE) and Nissl staining, immunofluorescence dual-labeling staining, and terminal deoxynucleotidyl transferase dUTP nick end labeling (TUNEL) staining. All sections were stored at -20 °C until they were utilized.

Hematoxylin-Eosin (HE) and Nissl Staining

HE and Nissl staining kits were purchased from Wanleibio (WLA051a, China) and Beyotime (C0117, China), respectively. All protocols were carried out as described previously [4,9]. Prepared sections were taken out of the -20 °C and air-dried for 3–4 h at room temperature (RT) following by conducting the following experiments. All finishing staining sections were finally observed and imaged using an optical microscope (BX43, Olympus, Japan) at a magnification of × 40 or × 100.

For HE Staining: All the procedures were adjusted as follows: Washing with deionized water for 5 min, staining with hematoxylin for 2 min and eosin for 15 s, respectively, dehydrating with 95% ethanol and clearing with xylene for 2 min twice respectively, and mounting finally with neutral gum.

For Nissl Staining: Sections were soaked in 100% ethanol and chloroform (1:1, v/v) overnight in the dark at RT. The day late, the sections were passed through 100% 95% ethanol, and deionized water for 1 min respectively following by being incubated in 37-50 °C pre-warmed crystal violet solution for 5 min. Subsequently, the sections were dehydrated in 100% ethanol and clearing with xylene for 5 min twice respectively and mounted finally using neutral gum. The number of Nissl-positive neurons was analyzed in four randomly selected areas of the ventral horn of spinal cords.

Quantitative Real-Time PCR (qRT-PCR) Analysis

Total RNA were isolated from rat spinal cord tissues using TRIzol^{TM} reagent (15596018, Invitrogen; ThermoFisher Scientific, Inc.) according to the manufacturer's protocols, the amount and purity of the mRNA extracts were determined by a spectrophotometry (DPI-1, Qiagen) based on the ratio of the optical density value measured under 260 nm and 280 nm. Subsequently, reverse transcription was performed to synthesize cDNA from 1 μg of total mRNA using the PrimeScript™ RT reagent Kit with gDNA Eraser (RR047A, TaKaRa, Otsu, Japan), and the qRT-PCR with TB Green® Premix Ex Taq™ II (RR820A, TaKaRa, Otsu, Japan) was conducted to quantify all the gene transcripts on the ABI StepOnePlus Real-Time PCR System (Thermo Fisher Scientific, CA, USA). The thermocycling conditions were adjusted as follows: initial denaturation (95°C, 30 s), 40 cycles for amplification reaction including denaturation (95°C, 5 s), annealing (60°C, 20 s) and extension (65°C, 15 s). The specified primers utilized in our present study were designed using the software Primer 6.0 (Applied Biosystems) based on the sequences obtained from Oligo 7 (Applied Biosystems) and displayed in **Table 1**. We evaluated the ratio of gene expression profiling by the threshold cycle (Ct) and used Glyceraldehyde 3-phosphate dehydrogenase (GAPDH) whose ΔΔCt value was set at 1 as the housekeeping gene. Finally, the relative mRNA expression levels of target genes were normalized to GAPDH and were calculated using the $2^{-\Delta\Delta Ct}$ method.

Table 1. List of primers for Quantitative Real-Time PCR

Targets genes (Accession Number)	Forward primer (5'-3')	Reverse primer (5'-3')
SIRT1 (NM_001372090.1)	ATAGGGAACCTCTGCCTCAT	CCACCTAACCTATGACACAACTC
AMPK (NM_023991.1)	GCTGACTTCGGACTCTCTAATATG	CATACAGCCTTCCTGAGATGAC
GAPDH (NM_017008.4)	GGTGGAAGAATGGGAGTTGCT	CTGGAGAAACCTGCCAAGTATG

Western Blotting Analysis

Proteins were extracted as our previous studies [4,9]. Briefly, 10 or 12% sodium dodecyl sulfate-polyacrylamide gel electrophoresis and 0.22 or 0.45 μm polyvinylidene fluoride membranes (Millipore, Germany) were performed to isolate and transblotted the protein, respectively. Afterwards, membranes were incubated with 5% non-fat dry milk to block the nonspecific binding sites for 2 h at RT followed by being incubated overnight at 4°C with anti-SIRT1 (#9475, 1:1000, Cell Signaling Technology),

anti-p-AMPK (AF3423, 1:800), anti-Beclin-1 (AF5128, 1:800), anti-LC3B (AF4650, 1:800), anti-Bcl-2 (AF6139, 1:800), anti-Bax (AF0120, 1:800), anti-Cleaved-caspase-3 (AF7022, 1:800) (all from Affinity, USA), anti-p62 (#23214, 1:1000), anti-Bcl-xL (#2762, 1:1000), anti-Bak (#3814, 1:000) (all from Cell Signaling Technology), and β-actin (sc-47778, 1:400, Santa Cruz Biotechnology, USA). The next day, they were further incubated with the corresponding secondary antibodies (7074P2/7074P6, 1:2000, Cell Signaling Technology) conjugated with horseradish peroxidase for 2 h at RT. The bands were visualized using an enhanced chemiluminescent reagents (ECL) (WKLS0l00, Millipore) and Image J software (Media Cybernetics, Georgia, MD, USA) was applied to analyze the grayscale value of protein.

Immunofluorescence Double Staining

All the procedures of staining were similar to our previous studies [4,9]. Briefly, the tissue sections were permeabilized with 0.3 % Triton X-100 for 15 min, and blocked with 5 % normal goat serum (005-000-121, Jackson) for 1 h at RT, and then were incubated with anti-Neuron (MAB377X, 1:50, Millipore), anti-Beclin-1 (AF5128, 1:100), and anti-LC3B (AF4650, 1:100) (all from Affinity, USA) overnight at 4℃. The following day, Sections were washed with 0.1% PBS (3 × 5 min) and incubated with the fluorescent secondary antibodies conjugated with Alexa Fluor 594 goat anti-mouse IgG (A-11005, 1:250) or Alexa Fluor 488 goat anti-rabbit IgG (A-11034, 1:250) (all from Thermo Fisher Scientific, USA) for 2 h at RT. Subsequently, sections were counterstained using 4',6-diamidino-2-phenylindole (DAPI) (D9542, 1:1000, Sigma-Aldrich) to label the nuclei for 8-10 min, and finally observed and photographed using a fluorescence microscope (IX51, Olympus, Japan) at 40 × magnification. Five different randomly visual fields were selected in each rat per group. Image processing software (Media Cybernetics Inc., Georgia, MD, USA) was used to count the number of Beclin-1-positive and LC3-positive cells in images randomly selected from each slide.

Terminal Dexynucleotidyl Transferase-mediated dUTP Nick End Labeling (TUNEL) Staining

Sections samples were stained using terminal deoxynucleotidyl transferase-mediated dUTP nick end labeling (TUNEL) apoptosis detection kit (KGA7071, Jiangsu KeyGEN BioTECH Corp, Jiangsu, China). All the procedures were performed according to the manufacturer's instructions. Briefly, sections were rinsed in 0.3% Triton X-100 for 5 min and subsequently incubated with 50 μL-TUNEL reaction mixture in the dark at RT. Afterwards, anti-Neuron (MAB377X, 1:50, Millipore) was added to the sections and incubated overnight at 4℃. The next day, sections were incubated with the fluorescent secondary antibody Alexa Fluor 594 (A-11005, 1:250, Thermo Fisher Scientific, USA) after being washed with 0.1% PBS (3 × 5 min) for 2 h at RT. Finally, sections were stained with DAPI for 10 min and observed using a fluorescence microscope (IX51, Olympus, Japan).

Transmission Electron Microscope (TEM)

Rats were sacrificed at 7 days post-surgery, and then a 0.5-cm long spinal cord sample centered the injured site was obtained after transcardial perfusion with 0.1M PBS, followed by fixation immediately with 2.5% glutaraldehyde and 1% osmium tetroxide overnight. Subsequently, dissected spinal cords were subjected to gradient alcohol dehydration, and then embedded in araldite overnight. Afterwards, ultrathin

sections (50 nm) were obtained using ultramicrotome (Leica ultracut UCT) and counterstained with uranyl acetate and lead citrate. Finally, images were captured with a transmission electron microscope (TEM) (HT7800, Hitachi, Japan) to evaluate the intracellular structure in neurons.

Statistical Analysis

Statistical analysis was performed using GraphPad Prism 8.0 Program (Graph Pad Software, San Diego, CA, USA). All the results were presented as mean ± standard error of the mean (SEM) and are representative of at least three independent experiments. Comparisons among groups using one-way analysis of variance (ANOVA) followed by Tukey's post-hoc Test under the premise of Parametric data (normality and equal variance passed), otherwise using Kruskal-Wallis ANOVA. The BBB rating scores were analyzed using two-factor ANOVA followed by Bonferroni post-hoc for repeated measures. $P < 0.05$ was considered statistically significant.

Results

OMT Benefited Locomotor Function Recovery after SCI

The protective effect of OMT on locomotor recovery of SCI rats was evaluated using both the average BBB scales at days 0, 1, 3, and 7, and footprint analysis at day 7 following SCI. As shown in **Fig. 1C**. The BBB scores of rats in the sham group were 21 at all four time points, but declined dramatically at day 1 and thereafter showed evidence of gradual improvements over time in the other treatment groups. Interestingly, OMT-treated rats exhibited markedly higher BBB scores compared with rats in the SCI group at day 3 ($P < 0.01$). These differences became even more pronounced at day 7 ($P < 0.001$), suggesting a better functional recovery of injured rats after treatment with OMT. However, this beneficial effect of OMT after SCI was partly abrogated after administration of SIRT1 inhibitor EX527 ($P < 0.05$) at day 7. In addition, this improvement in functional recovery following OMT treatment was observed in the footprint analysis (**Fig. 1D**). Rats in the sham group showed fairly coordinated movements of the fore- and hindlimbs without hind limb dragging, while injured animals at day 7 exhibited extensive dragging of hind limbs and inconsistent coordination in hind paw stepping. Conversely, those rats treated with OMT displayed a marked recovery of gait, characterized with clear hindlimb coordination and little toe dragging. Again, the therapeutic effect of OMT on gait was significantly inhibited by co-treatment with EX527. All the above results indicated that OMT contributed to functional recovery of rats with SCI.

OMT Ameliorated Tissue Damage and Reduced the Loss of Locomotor Neurons after SCI

We next performed HE staining to observe the size of damaged spinal cords at day 7 post SCI (**Fig. 2A**). SCI caused structural damage to the spinal cord, with large and irregular cavities compared with the sham group. In the OMT group, the lesion area was significantly smaller, indicating that OMT could ameliorate tissue damage following SCI. To determine the effect of OMT on neuronal survival, we utilized Nissl staining to count ventral horn motor neurons around the injured epicenter. Rats in the SCI group had fewer neurons with irregular neuronal structures in spinal cords compared with the sham group ($P <$

0.001, **Fig. 2B and C**). After treatment with OMT or co-treatment with EX527, rats exhibited a significantly increased number of surviving neurons ($P < 0.001$, $P < 0.05$, **Fig. 2B and C**) and showed improved neuronal morphology, while the number of surviving neurons was significantly decreased in the OMT-EX527 co-treatment group compared with the OMT-only group ($P < 0.05$, **Fig. 2B and C**). This observation suggested that OMT promoted neuronal survival after SCI in rats.

OMT Activates the SIRT1/AMPK Signaling Pathway after SCI

AMPK is a direct downstream target protein of SIRT1 against SCI [31,32]. To investigate the effects of OMT treatment on the SIRT1/AMPK signaling pathway following SCI in rats, we performed Western blotting and qRT-PCR to examine the expression of SIRT1 and phosphorylated AMPK (p-AMPK) at day 7 after SCI. In the protein analysis of band density, levels of SIRT1 ($P < 0.01$, **Fig. 3A and B**) and p-AMPK ($P < 0.01$, **Fig. 3A and C**) expression were significantly increased after injury compared with the sham group, suggesting SCI induced activation of the SIRT1/AMPK signaling pathway. Compared with the SCI group, the protein expression of SIRT1 and p-AMPK was higher in the OMT group ($P < 0.05$, $P < 0.01$, **Fig. 3A-C**). Importantly, EXT527 treatment resulted in a significantly lower expression of these proteins ($P < 0.01$, $P < 0.01$, **Fig. 3A-C**) compared with the OMT group. qRT-PCR revealed that the mRNA expression levels of SIRT1 and AMPK in the injured spinal cord were increased in the SCI group in comparison to the Sham group ($P < 0.05$, $P < 0.05$, **Fig. 3D and E**). Levels of SIRT1 and p-AMPK were significant higher in the OMT-treated group compared to both the SCI group and the EX527 group ($P < 0.01$, $P < 0.01$, **Fig. 3D and E**), indicating that OMT treatment could significantly promote expression of SIRT1 and p-AMPK, while co-treatment with SIRT1 inhibitor EX527effectively inhibited SIRT1 and p-AMPK expression ($P < 0.05$, $P < 0.001$, **Fig. 3D and E**).

OMT Promotes the Neuronal Autophagy after SCI

To determine the effect of OMT treatment on neuronal autophagy after SCI in rats, we performed Western blotting to assess expression levels of the proteins p62, Beclin-1, and microtubule-associated protein 1 light chain 3B (MAP1LC3B, hereafter referred to LC3B), which are well-established indicators of cellular autophagy [51-53] in the injured spinal cords. At day 7 after SCI, levels of p62 ($P < 0.001$, **Fig. 4A and B**), Beclin-1 ($P < 0.01$, **Fig. 4A and C**) and LC3B ($P < 0.01$, **Fig. 4A and D**) expression were significantly increased compared with the sham group, indicating an induction of autophagy after SCI. It is worthwhile to note that level of p62 expression was significantly lower, whereas those of Beclin-1 and LC3B were remarkably higher in OMT-treated rats compared with the SCI group ($P < 0.01$, $P < 0.01$, $P < 0.01$, **Fig. 4A-D**), suggesting that OMT treatment elicited enhanced autophagic flux following SCI in rats.

To further confirm these findings, we employed immunofluorescence double staining (Beclin-1/Neuron and LC3B/Neuron) to evaluate the activity of autophagy in neurons in the ventral horn of the spinal cords around the injured area in rats. Consistent with the results of Western blotting, the number of both Beclin-1-positive neurons ($P < 0.01$, **Fig. 4E and F**) and LC3B-positive neurons ($P < 0.05$, **Fig. 4G and H**) was significantly higher at day 7 after the injury compared with the sham group. In the OMT-treated group rats,

Beclin-1 and LC3B-positive neurons were significantly elevated compared with rats in the SCI group (P < 0.001, P < 0.001) and EX527 group (P < 0.01, P < 0.01) (**Fig. 4E-H**), suggesting that the neuronal autophagy was significantly increased after SCI and OMT administration greatly promotes neuronal autophagy following injury via the SIRT1/AMPK signaling pathway.

OMT Suppresses the Neuronal Apoptosis after SCI

Autophagy has been reported to reduce neuronal cell death following SCI in rats [5]. To investigate the effect of OMT on neuronal apoptosis via autophagy, we performed Western blotting to examine the expression levels of Bcl-2 and Bcl-xL, known for their anti-apoptotic effect [54,55] , and Cleaved-caspase-3 (C-caspase-3) [56], Bax and Bak, known for their pro-apoptotic effects [57,58], at day 7 after SCI. We observed a significantly decreased expression of Bcl-2 (P < 0.05, **Fig. 5A and B**) and Bcl-xL (P < 0.05, **Fig. 5F and G**), and significantly increased expression of Bax (P < 0.05, **Fig. 5A and C**), C-caspase-3 (P < 0.001, **Fig. 5A and E**) and Bak (P < 0.001, **Fig. 5F and H**), as well as the ratio of Bax/Bcl-2 (P < 0.001, **Fig. 5A and D**) following injury compared with the sham group, again highlighting elevated levels of cell death after SCI. However, OMT administration resulted in a significant increase of Bcl-2 and Bcl-xL, and reduction of Bax, C-caspase-3, Bak and the ratio of Bax/Bcl-2 levels compared with both the untreated SCI group (P < 0.001 or P < 0.05, **Fig. 5A-H**) and co-treated EX527 group (P < 0.05 or P < 0.01, **Fig. 5A-H**), suggesting that OMT promotes the inhibition of cellular apoptosis following SCI in rats.

To locate apoptotic neurons, we performed TUNEL staining with neuronal co-staining to quantify the number of apoptotic neurons in the injured area. After SCI at day 7, The number of TUNEL-positive (apoptotic) neurons were significantly higher than in the sham group (P < 0.001, **Fig. 5I and J**), indicating the impairment of neurons following injury, but this increase in TUNEL-positive cells could be rescued by OMT treatment (P < 0.001, **Fig. 5I and J**). Interestingly, co-treatment of OMT with EX527 group (P < 0.01, **Fig. 5I and J**) also resulted in fewer TUNEL-positive than untreated SCI. However, the number of TUNEL-positive cells was significantly lower in the OMT-only-treated group compared with the OMT-EX527-co-treated group (P < 0.05, **Fig. 5I and J**). Taken together, the above results demonstrated that OMT substantially suppressed neuronal apoptosis in a rat model of SCI, and the protective effects are partly mediated via activation of the SIRT1/AMPK signaling pathway.

OMT Improves the Neuronal Ultrastructures after SCI

To further confirm the improving effect of OMT on spinal cord neurons at day 7 after SCI, we performed TEM to observe the ultrastructural changes of neurons among groups **(Fig. 6)**. Notably, no detected autophagosomes in the sham group whose rats exhibited intact neuronal intracellular structure as showed by regular nuclei and normal mitochondria with distinct crista. In contrast, in the SCI-group rats, neurons displayed obvious cellular damages characterized by karyotin pyknosis and margination, cytoplasm vacuolization, as well as mitochondrial swelling. In addition, increased autophagosomes numbers were observed in the neurons. However, the morphological impairments in neurons of SCI models were significantly alleviated to some extent, and along with remarkably increased

autophagosomes when single treatment of OMT or co-treatment of OMT with EXT527. Collectively, these data indicated that the OMT treatment could effectively enhance autophagy and attenuate the structural impairments of neurons following SCI in rats.

Discussion

SCI is well known as a devastating central nervous system trauma characterized by high morbidity and long-term disability, placing a heavy burden on families, healthcare systems, and society overall [59]. OMT is a major quinolizidine alkaloid extracted from the root of *Sophora flavescens Ait* and has previously been reported to exert anti-inflammatory, anti-apoptotic, and anti-antioxidant functions, with a potential protective effect against ischemia or ischemia/reperfusion injuries of brain in rats [60, 45, 61]. However, the protective effects and molecular mechanisms underlying OMT action following SCI remain unknown. In the present study, we demonstrated that OMT significantly reduced neural tissue damage, inhibited neuronal apoptosis and promoted survival of neurons, and ultimately improved functional recovery in a rat model of compressive SCI. Furthermore, our data also provides evidence that the therapeutic efficiency of OMT involves the enhancement of neuronal autophagy activity mediated by the SIRT1/AMPK signaling pathway, revealing a novel molecular basis for the neuroprotective role of OMT. Taken together, this is the first study to date that we investigated the link between OMT-mediated neuroprotection and neuronal autophagy, and explored the specific molecular mechanisms of the beneficial effects of OMT following SCI in rats. Our data imply that OMT treatment may represent a potential and effective therapeutic strategy against SCI in the future.

Locomotor dysfunction is the characteristic hallmark of SCI and is attributed to the damage of locomotor neurons [8]. Apoptosis, a cascade cleaving process of proteinase, has been recognized to be one main forms of neuronal loss following SCI. Mounting studies have reported that inhibition of apoptosis in neurons resulted in positive effects towards the functional recovery of SCI in rats [62, 6, 63]. Apoptosis-induced cell death is governed by a large number of genes, including Caspase-3, a key mediator of cell death, which is reported to be involved in the final execution of apoptosis phase and Bax, Bak and Bcl-2, Bcl-xL (four main members of Bcl-2 family) [54, 57]. Caspase-3 is activated following translocation of the pro-apoptotic protein Bax and Bak from the cytoplasm to the mitochondria, ultimately leading to nuclear damage and DNA fragmentation [56]. Contrarily, Bcl-2 and Bcl-xL, considered as a key anti-apoptotic factor, can effectively counteract the pro-apoptotic effects of Bax and Bak, further maintain the cellular homeostasis. An upregulation of the expression of Bcl-2 and Bcl-xL is thought to indicate an inhibition of apoptosis [55, 64]. Autophagy, a main intracellular catabolic process for the degradation of cytoplasmic proteins and organelles, plays a major role in the occurrence and progression of secondary SCI [20, 21]. Accumulating evidence has revealed the importance of autophagy as same as apoptosis and demonstrated that autophagy occurs prior to apoptosis in the process of neuronal cell death following secondary SCI [5].

Previous studies have reported that autophagy can act as “double-edged sword”, exhibiting both beneficial or detrimental roles for neuronal survival depending on the location and severity of neuronal injury. In some injury models of the brain [65, 66] and spinal cord [67], the enhancement of autophagy results in cell death and contributes to functional outcome deficits. Conversely, autophagy can also effectively suppress apoptosis by clearing damaged organelles, further alleviating neuronal death in response to the CNS disorders. For example, after brain injury, Ding et al. [68] and Zhang et al. [69] detected the changes of autophagy-labeled proteins Beclin-1-associated with autophagosome activity [52] and LC3B -involved in autophagosome formation [53], whose upregulated expression implied the activation of autophagy, and revealed a protective role of autophagy for promoting neuronal survival and inhibiting neuronal degeneration. Additionally, Li et al. [1] and Li et al. [62] also reported that SCI triggered autophagy, and enhanced autophagy activity induced by exendin-4 and curcumin could protect neurons from damage and benefit the recovery of neurological functions by inhibiting neuronal apoptosis in a rat model of acute SCI. Consistently, autophagy inhibition resulted in neuronal damage and neurodegeneration in mice [70]. These findings are strongly in agreement with our present results. In this study, we found that the protein levels of Beclin-1 and LC3B expression were significantly elevated after SCI, and were moreover significantly higher after OMT treatment. Similarly, the number of Beclin-1 and LC3B positive neurons was found to be significantly increased in immunofluorescence staining, which was further dramatically increased in OMT-treated rats after 7 days post injury. p62, known as autophagic degradation substrate, is widely used as a marker of autophagic flux [51]. Studies have demonstrated that p62 protein interacts with LC3B and involves in the formation and degradation of autophagosomes. Accumulation of p62 protein indicates the blockage of the autophagy degradation and downregulation of p62 expression represents the enhancement of autophagic flux [71]. Here, our study revealed that p62 protein expression was significantly increased at day 7 after SCI, and dramatically decreased after treatment with OMT, suggesting that OMT accelerates activation of a whole autophagic flux. Similar results were evidenced by increased autophagosomes observed in the OMT-treated group compared to the SCI group by TEM. Together, these data suggested that OMT could effectively enhance SCI-induced neuronal autophagy. Importantly, we also found that OMT significantly reduced the expression of C-caspase-3, Bax and Bak proteins, as well as the ratio of Bax/Bcl2, while increasing the level of Bcl-2 and Bcl-xL expression following SCI in rats. TUNEL and Nissl staining confirmed that OMT treatment notably increased the number of surviving neurons after SCI, while inhibiting the proportion of apoptotic neurons. In addition, TEM results showed that SCI surgery led to obvious neuronal subcellular structural damage manifested by abnormal nuclei and a proportion of mitochondrial vacuolization, indicating induction of neuronal apoptosis following compression-induced SCI in rats, but treatment with OMT or co-treatment with EX527 could significantly improve the intracellular morphological impairments of neurons and reverse these phenomena to some extent. These data implied that, at least in part, OMT could significantly inhibit SCI-induced neuronal apoptosis which may be associated with its promotion of autophagy activity in rats.

To further clarify the protective role of OMT following SCI in rats, we utilized the BBB scores and HE staining to investigate the locomotor recovery of SCI rats and the morphological changes of spinal cord

tissue. Obviously, OMT treatment significantly improved locomotor functions compared with untreated rats subjected to SCI. Moreover, our histopathological results revealed that OMT markedly alleviated tissue damage in the injured spinal cord. The results clearly indicate a positive effect of OMT after SCI in rats.

SIRT1 is known as a conserved nicotinamide adenine dinucleotide (NAD+)-dependent histone deacetylase. Numerous previous studies have demonstrated an active involvement of SIRT1 in cellular metabolism, autophagy, apoptosis, inflammation, oxidative stress and aging [27–30]. AMP-activated protein kinase (AMPK) is generally considered as a stress response enzyme and its activation can induce the promotion of autophagy in various of CNS diseases [72, 6]. Previous studies have revealed a role for AMPK as a direct downstream target protein of SIRT1 after SCI. Zhao et al. [31] have demonstrated that SIRT1 activator resveratrol could target activated AMPK to promote neuronal autophagy, thereby improving the neurological functional recovery following SCI in rats. Moreover, Gao et al. [32] found that melatonin could trigger neuronal autophagy and inhibit apoptosis via activation of the SIRT1/AMPK signaling pathway in rat models of SCI. These findings identified the neuroprotective role of the SIRT1/AMPK signaling pathway in regulating the neuronal autophagy and apoptosis following SCI in rats. Interestingly, OMT has been reported to attenuate hippocampal ischemia/reperfusion injury via upregulation of SIRT1 and thereby influencing the processes of autophagy and apoptosis [46]. All of the above evidence prompted us to investigate whether OMT targets the SIRT1/AMPK signaling pathway to promote autophagy and inhibit apoptosis following SCI in rats. To confirm our hypothesis, we utilized EX527, a specific inhibitor of SIRT1, to investigate the relationship between SCI-induced enhanced autophagy and the SIRT1/AMPK signaling pathway. Following SCI and subsequently used Western blotting and qRT-PCR to detect protein and gene expression of SIRT1 and p-AMPK, we found that both SIRT1 and p-AMPK were significantly upregulated at 7 days, Interestingly, their expression was further increased after OMT administration, suggesting that OMT further promoted the SIRT1/AMPK signal pathway activation following SCI in rats. In addition, Western blotting or immunofluorescence results revealed changes in representative autophagy biomarkers Beclin-1 and LC3B, as well as apoptosis-related factors Bax, C-caspase-3, and Bcl-2 in neurons. EX527 treatment resulted in a significant suppression of autophagy activity following OMT treatment and abrogated the beneficial effects of OMT treatment on suppression of neuronal apoptosis, indicating that OMT promoted autophagy via activation of the SIRT1/AMPK signaling pathway. However, the neuroprotective effects of OMT were not entirely blocked by EX527, which indicates that there could be other underlying mechanisms involved in neuroprotection of OMT after SCI.

In conclusion, our present study demonstrates for the first time that OMT significantly inhibits SCI-induced neuronal apoptosis and promotes functional recovery of rat hindlimbs. The protective effects of OMT are related to the enhancement of autophagy in neuronal cells via activation of the SIRT1/AMPK signaling pathway (Fig. 7). Therefore, our results indicate a new potential mechanism which represents another property of OMT in neuroprotection following SCI, and OMT may be considered as a promising therapeutic strategy against SCI in the future. Next, we will conduct the further clinical study to determine

the protective roles of OMT against SCI in humans. However, there are several limitations that should be considered in the interpretation of our results. Firstly, while a single dose of OMT (40 mg/kg) was reported to exert protective effects against SCI, it is necessary to clarify the optimal dose and therapeutic window. Secondly, based on the time limitations, we harvested animals at day 7 following SCI, which did not enable us to explore the long-term effects of OMT on SCI. Lastly, as inhibition of autophagy by EX527 only partly prevented the effects of OMT on neuronal apoptosis, the other possible pathophysiological mechanisms will need to be further investigated in vitro in the future.

Abbreviations

SCI	Spinal cord injury
OMT	Oxymatrine
BBB	Basso, Beattie, and Bresnahan
CNS	Central nervous system
SIRT1	Silent information regulator 1
AMPK	AMP-activated protein kinase
HE	Hematoxylin-eosin
PBS	Phosphate-buffered saline
TUNEL	Terminal deoxynucleotidyl transferase-mediated dUTP nick end labeling
DAPI	4',6-diamidino-2-phenylindole
MAP1LC3B	Microtubule-associated protein 1 light chain 3B
TEM	Transmission electron microscope

Declarations

Acknowledgements

This work was financially supported by the 2021 Youth Science and Technology Talents Support Plan from Boze Project of Jinzhou Medical University (Grant No: JYBZQT2111), the National Natural Science Foundation of China (Grant No: 81501659), the Science Research Class of Liaoning Provincial Education Department (Grant No: JYTJCZR201911), the Natural Science Foundation of Liaoning Province (Grant No: 2020-MS-298), and the Science Research Foundation of Qilu Hospital of Shandong University (Qingdao) (Grant No: QDKY2020BS01).

Author Contributions

JL and ZF conceived and designed the study; YC, YW, and GL provided the technical support; JL and LL analyzed the data; XC, JC, and SM assisted for animals care; JL wrote and revised the primary manuscript; JL, YW, ZF and GL afforded the funding sources. All authors read and approved the final manuscript.

Compliance with Ethical Standards

Ethics Approval and Consent to Participate

Not applicable.

Consent for Publication

Not applicable.

Availability of Data and Materials

All data are real and guarantee the validity of results and are available from the authors upon request.

Conflicts of Interest

The authors declare that there are no competing financial interest.

References

1. Li HT, Zhao XZ, Zhang XR, Li G, Jia ZQ, Sun P, Wang JQ, Fan ZK, Lv G (2016) Exendin-4 Enhances Motor Function Recovery via Promotion of Autophagy and Inhibition of Neuronal Apoptosis After Spinal Cord Injury in Rats. Mol Neurobiol 53 (6):4073-4082. doi:10.1007/s12035-015-9327-7
2. Oyinbo CA (2011) Secondary injury mechanisms in traumatic spinal cord injury: a nugget of this multiply cascade. Acta Neurobiol Exp (Wars) 71 (2):281-299
3. Sun L, Li M, Ma X, Zhang L, Song J, Lv C, He Y (2019) Inhibiting High Mobility Group Box-1 Reduces Early Spinal Cord Edema and Attenuates Astrocyte Activation and Aquaporin-4 Expression after Spinal Cord Injury in Rats. J Neurotrauma 36 (3):421-435. doi:10.1089/neu.2018.5642
4. Li J, Jia Z, Xu W, Guo W, Zhang M, Bi J, Cao Y, Fan Z, Li G (2019) TGN-020 alleviates edema and inhibits astrocyte activation and glial scar formation after spinal cord compression injury in rats. Life Sciences 222:148-157. doi:10.1016/j.lfs.2019.03.007
5. Tang P, Hou H, Zhang L, Lan X, Mao Z, Liu D, He C, Du H, Zhang L (2014) Autophagy reduces neuronal damage and promotes locomotor recovery via inhibition of apoptosis after spinal cord injury in rats. Mol Neurobiol 49 (1):276-287. doi:10.1007/s12035-013-8518-3
6. Wu C, Chen H, Zhuang R, Zhang H, Wang Y, Hu X, Xu Y, Li J, Li Y, Wang X, Xu H, Ni W, Zhou K (2021) Betulinic acid inhibits pyroptosis in spinal cord injury by augmenting autophagy via the AMPK-mTOR-TFEB signaling pathway. Int J Biol Sci 17 (4):1138-1152. doi:10.7150/ijbs.57825

7. Rong Y, Liu W, Wang J, Fan J, Luo Y, Li L, Kong F, Chen J, Tang P, Cai W (2019) Neural stem cell-derived small extracellular vesicles attenuate apoptosis and neuroinflammation after traumatic spinal cord injury by activating autophagy. Cell Death Dis 10 (5):340. doi:10.1038/s41419-019-1571-8
8. Ren XD, Wan CX, Niu YL (2019) Overexpression of lncRNA TCTN2 protects neurons from apoptosis by enhancing cell autophagy in spinal cord injury. FEBS Open Bio 9 (7):1223-1231. doi:10.1002/2211-5463.12651
9. Li J, Jia Z, Zhang Q, Dai J, Kong J, Fan Z, Li G (2021) Inhibition of ERK1/2 phosphorylation attenuates spinal cord injury induced astrocyte activation and inflammation through negatively regulating aquaporin-4 in rats. Brain Res Bull 170:162-173. doi:10.1016/j.brainresbull.2021.02.014
10. Guan B, Chen R, Zhong M, Liu N, Chen Q (2020) Protective effect of Oxymatrine against acute spinal cord injury in rats via modulating oxidative stress, inflammation and apoptosis. Metab Brain Dis 35 (1):149-157. doi:10.1007/s11011-019-00528-8
11. Gokce EC, Kahveci R, Gokce A, Cemil B, Aksoy N, Sargon MF, Kisa U, Erdogan B, Guvenc Y, Alagoz F, Kahveci O (2016) Neuroprotective effects of thymoquinone against spinal cord ischemia-reperfusion injury by attenuation of inflammation, oxidative stress, and apoptosis. J Neurosurg Spine 24 (6):949-959. doi:10.3171/2015.10.SPINE15612
12. Fakhri S, Abbaszadeh F, Moradi SZ, Cao H, Khan H, Xiao J (2022) Effects of Polyphenols on Oxidative Stress, Inflammation, and Interconnected Pathways during Spinal Cord Injury. Oxid Med Cell Longev 2022:8100195. doi:10.1155/2022/8100195
13. Nagai J, Kitamura Y, Owada K, Yamashita N, Takei K, Goshima Y, Ohshima T (2015) Crmp4 deletion promotes recovery from spinal cord injury by neuroprotection and limited scar formation. Sci Rep 5:8269. doi:10.1038/srep08269
14. Wang C, Liu C, Gao K, Zhao H, Zhou Z, Shen Z, Guo Y, Li Z, Yao T, Mei X (2016) Metformin preconditioning provide neuroprotection through enhancement of autophagy and suppression of inflammation and apoptosis after spinal cord injury. Biochem Biophys Res Commun 477 (4):534-540. doi:10.1016/j.bbrc.2016.05.148
15. Huang H, Young W, Skaper S, Chen L, Moviglia G, Saberi H, Al-Zoubi Z, Sharma HS, Muresanu D, Sharma A, El Masry W, Feng S, International Association of N, The Chinese Association of N (2020) Clinical Neurorestorative Therapeutic Guidelines for Spinal Cord Injury (IANR/CANR version 2019). J Orthop Translat 20:14-24. doi:10.1016/j.jot.2019.10.006
16. Xue M, Yong VW (2020) Neuroinflammation in intracerebral haemorrhage: immunotherapies with potential for translation. Lancet Neurol 19 (12):1023-1032. doi:10.1016/S1474-4422(20)30364-1
17. Shah M, Peterson C, Yilmaz E, Halalmeh DR, Moisi M (2020) Current advancements in the management of spinal cord injury: A comprehensive review of literature. Surg Neurol Int 11:2. doi:10.25259/SNI_568_2019
18. Li Y, Han W, Wu Y, Zhou K, Zheng Z, Wang H, Xie L, Li R, Xu K, Liu Y, Wang X, Xiao J (2019) Stabilization of Hypoxia Inducible Factor-1alpha by Dimethyloxalylglycine Promotes Recovery from

Acute Spinal Cord Injury by Inhibiting Neural Apoptosis and Enhancing Axon Regeneration. J Neurotrauma 36 (24):3394-3409. doi:10.1089/neu.2018.6364

19. Mizushima N (2007) Autophagy: process and function. Genes Dev 21 (22):2861-2873. doi:10.1101/gad.1599207
20. Kanno H, Ozawa H, Sekiguchi A, Itoi E (2009) The role of autophagy in spinal cord injury. Autophagy 5 (3):390-392. doi:10.4161/auto.5.3.7724
21. Klionsky DJ (2014) Coming soon to a journal near you - the updated guidelines for the use and interpretation of assays for monitoring autophagy. Autophagy 10 (10):1691. doi:10.4161/auto.36187
22. Fernandez A, Ordonez R, Reiter RJ, Gonzalez-Gallego J, Mauriz JL (2015) Melatonin and endoplasmic reticulum stress: relation to autophagy and apoptosis. J Pineal Res 59 (3):292-307. doi:10.1111/jpi.12264
23. Wnuk A, Kajta M (2017) Steroid and Xenobiotic Receptor Signalling in Apoptosis and Autophagy of the Nervous System. Int J Mol Sci 18 (11). doi:10.3390/ijms18112394
24. Wu J, Lipinski MM (2019) Autophagy in Neurotrauma: Good, Bad, or Dysregulated. Cells 8 (7). doi:10.3390/cells8070693
25. Lipinski MM, Wu J, Faden AI, Sarkar C (2015) Function and Mechanisms of Autophagy in Brain and Spinal Cord Trauma. Antioxid Redox Signal 23 (6):565-577. doi:10.1089/ars.2015.6306
26. Houtkooper RH, Pirinen E, Auwerx J (2012) Sirtuins as regulators of metabolism and healthspan. Nat Rev Mol Cell Biol 13 (4):225-238. doi:10.1038/nrm3293
27. Zhang Y, Cao X, Zhu W, Liu Z, Liu H, Zhou Y, Cao Y, Liu C, Xie Y (2016) Resveratrol Enhances Autophagic Flux and Promotes Ox-LDL Degradation in HUVECs via Upregulation of SIRT1. Oxid Med Cell Longev 2016:7589813. doi:10.1155/2016/7589813
28. Hu T, Chen Y, Jiang Q, Lin J, Li H, Wang P, Feng L (2017) Overexpressed eNOS upregulates SIRT1 expression and protects mouse pancreatic beta cells from apoptosis. Exp Ther Med 14 (2):1727-1731. doi:10.3892/etm.2017.4669
29. Velagapudi R, El-Bakoush A, Lepiarz I, Ogunrinade F, Olajide OA (2017) AMPK and SIRT1 activation contribute to inhibition of neuroinflammation by thymoquinone in BV2 microglia. Mol Cell Biochem 435 (1-2):149-162. doi:10.1007/s11010-017-3064-3
30. Lee IC, Ho XY, George SE, Goh CW, Sundaram JR, Pang KKL, Luo W, Yusoff P, Sze NSK, Shenolikar S (2018) Oxidative stress promotes SIRT1 recruitment to the GADD34/PP1alpha complex to activate its deacetylase function. Cell Death Differ 25 (2):255-267. doi:10.1038/cdd.2017.152
31. Zhao H, Chen S, Gao K, Zhou Z, Wang C, Shen Z, Guo Y, Li Z, Wan Z, Liu C, Mei X (2017) Resveratrol protects against spinal cord injury by activating autophagy and inhibiting apoptosis mediated by the SIRT1/AMPK signaling pathway. Neuroscience 348:241-251. doi:10.1016/j.neuroscience.2017.02.027
32. Gao K, Niu J, Dang X (2020) Neuroprotection of melatonin on spinal cord injury by activating autophagy and inhibiting apoptosis via SIRT1/AMPK signaling pathway. Biotechnol Lett 42

(10):2059-2069. doi:10.1007/s10529-020-02939-5

33. Wang S, Huang Y, Luo G, Yang X, Huang W (2021) Cyanidin-3-O-glucoside attenuates high glucose-induced podocyte dysfunction by inhibiting apoptosis and promoting autophagy via activation of SIRT1/AMPK pathway. Can J Physiol Pharmacol 99 (6):589-598. doi:10.1139/cjpp-2020-0341
34. Liang L, Huang J (2016) Oxymatrine inhibits epithelial-mesenchymal transition through regulation of NF-kappaB signaling in colorectal cancer cells. Oncol Rep 36 (3):1333-1338. doi:10.3892/or.2016.4927
35. Zhang Y, Piao B, Zhang Y, Hua B, Hou W, Xu W, Qi X, Zhu X, Pei Y, Lin H (2011) Oxymatrine diminishes the side population and inhibits the expression of beta-catenin in MCF-7 breast cancer cells. Med Oncol 28 Suppl 1:S99-107. doi:10.1007/s12032-010-9721-y
36. Ma SC, Du J, But PP, Deng XL, Zhang YW, Ooi VE, Xu HX, Lee SH, Lee SF (2002) Antiviral Chinese medicinal herbs against respiratory syncytial virus. J Ethnopharmacol 79 (2):205-211. doi:10.1016/s0378-8741(01)00389-0
37. Fan H, Li L, Zhang X, Liu Y, Yang C, Yang Y, Yin J (2009) Oxymatrine downregulates TLR4, TLR2, MyD88, and NF-kappaB and protects rat brains against focal ischemia. Mediators Inflamm 2009:704706. doi:10.1155/2009/704706
38. Jiang H, Meng F, Li J, Sun X (2005) Anti-apoptosis effects of oxymatrine protect the liver from warm ischemia reperfusion injury in rats. World J Surg 29 (11):1397-1401. doi:10.1007/s00268-005-7885-y
39. Jiang G, Liu X, Wang M, Chen H, Chen Z, Qiu T (2015) Oxymatrine ameliorates renal ischemia-reperfusion injury from oxidative stress through Nrf2/HO-1 pathway. Acta Cir Bras 30 (6):422-429. doi:10.1590/S0102-865020150060000008
40. Li Y, Yu P, Fu W, Cai L, Yu Y, Feng Z, Wang Y, Zhang F, Yu X, Xu H, Sui D (2021) Ginseng-Astragalus-oxymatrine injection ameliorates cyclophosphamide-induced immunosuppression in mice and enhances the immune activity of RAW264.7 cells. J Ethnopharmacol 279:114387. doi:10.1016/j.jep.2021.114387
41. Xiang X, Wang G, Cai X, Li Y (2002) Effect of oxymatrine on murine fulminant hepatitis and hepatocyte apoptosis. Chin Med J (Engl) 115 (4):593-596
42. Hong-Li S, Lei L, Lei S, Dan Z, De-Li D, Guo-Fen Q, Yan L, Wen-Feng C, Bao-Feng Y (2008) Cardioprotective effects and underlying mechanisms of oxymatrine against Ischemic myocardial injuries of rats. Phytother Res 22 (7):985-989. doi:10.1002/ptr.2452
43. Zhu B, Yang JR, Chen SF, Jiang YQ (2014) The attenuation of lung ischemia reperfusion injury by oxymatrine. Cell Biochem Biophys 70 (1):333-336. doi:10.1007/s12013-014-9917-4
44. Zhao J, Yu S, Tong L, Zhang F, Jiang X, Pan S, Jiang H, Sun X (2008) Oxymatrine attenuates intestinal ischemia/reperfusion injury in rats. Surg Today 38 (10):931-937. doi:10.1007/s00595-008-3785-8
45. Cui L, Zhang X, Yang R, Wang L, Liu L, Li M, Du W (2011) Neuroprotection and underlying mechanisms of oxymatrine in cerebral ischemia of rats. Neurol Res 33 (3):319-324. doi:10.1179/016164110X12759951866876

46. Zhou S, Qiao B, Chu X, Kong Q (2018) Oxymatrine attenuates cognitive deficits through SIRT1-mediated autophagy in ischemic stroke. J Neuroimmunol 323:136-142. doi:10.1016/j.jneuroim.2018.06.018
47. Ropper AE, Zeng X, Anderson JE, Yu D, Han I, Haragopal H, Teng YD (2015) An efficient device to experimentally model compression injury of mammalian spinal cord. Exp Neurol 271:515-523. doi:10.1016/j.expneurol.2015.07.012
48. Zheng XW, Shan CS, Xu QQ, Wang Y, Shi YH, Wang Y, Zheng GQ (2018) Buyang Huanwu Decoction Targets SIRT1/VEGF Pathway to Promote Angiogenesis After Cerebral Ischemia/Reperfusion Injury. Front Neurosci 12:911. doi:10.3389/fnins.2018.00911
49. Basso DM, Beattie MS, Bresnahan JC (1995) A sensitive and reliable locomotor rating scale for open field testing in rats. J Neurotrauma 12 (1):1-21. doi:10.1089/neu.1995.12.1
50. Kunkel-Bagden E, Dai HN, Bregman BS (1993) Methods to assess the development and recovery of locomotor function after spinal cord injury in rats. Exp Neurol 119 (2):153-164. doi:10.1006/exnr.1993.1017
51. Zhu N, Ruan J, Yang X, Huang Y, Jiang Y, Wang Y, Cai D, Geng Y, Fang M (2020) Triptolide improves spinal cord injury by promoting autophagy and inhibiting apoptosis. Cell Biol Int 44 (3):785-794. doi:10.1002/cbin.11273
52. Kanno H, Ozawa H, Sekiguchi A, Itoi E (2009) Spinal cord injury induces upregulation of Beclin 1 and promotes autophagic cell death. Neurobiol Dis 33 (2):143-148. doi:10.1016/j.nbd.2008.09.009
53. Weidberg H, Shpilka T, Shvets E, Abada A, Shimron F, Elazar Z (2011) LC3 and GATE-16 N termini mediate membrane fusion processes required for autophagosome biogenesis. Dev Cell 20 (4):444-454. doi:10.1016/j.devcel.2011.02.006
54. Yang J, Liu X, Bhalla K, Kim CN, Ibrado AM, Cai J, Peng TI, Jones DP, Wang X (1997) Prevention of apoptosis by Bcl-2: release of cytochrome c from mitochondria blocked. Science 275 (5303):1129-1132. doi:10.1126/science.275.5303.1129
55. Shim S, Kim S, Kwon YB, Kwon J (2012) Protection by [6]-shogaol against lipopolysaccharide-induced toxicity in murine astrocytes is related to production of brain-derived neurotrophic factor. Food Chem Toxicol 50 (3-4):597-602. doi:10.1016/j.fct.2011.11.042
56. Han W, Sun Y, Wang X, Zhu C, Blomgren K (2014) Delayed, long-term administration of the caspase inhibitor Q-VD-OPh reduced brain injury induced by neonatal hypoxia-ischemia. Dev Neurosci 36 (1):64-72. doi:10.1159/000357939
57. Wei MC, Zong WX, Cheng EH, Lindsten T, Panoutsakopoulou V, Ross AJ, Roth KA, MacGregor GR, Thompson CB, Korsmeyer SJ (2001) Proapoptotic BAX and BAK: a requisite gateway to mitochondrial dysfunction and death. Science 292 (5517):727-730. doi:10.1126/science.1059108
58. Sozbilen MC, Ozturk M, Kaftan G, Dagci T, Ozyalcin H, Armagan G (2018) Neuroprotective Effects of C-terminal Domain of Tetanus Toxin on Rat Brain Against Motorneuron Damages After Experimental Spinal Cord Injury. Spine (Phila Pa 1976) 43 (6):E327-E333. doi:10.1097/BRS.0000000000002357

59. Zhong L, Zhang H, Ding ZF, Li J, Lv JW, Pan ZJ, Xu DX, Yin ZS (2020) Erythropoietin-Induced Autophagy Protects Against Spinal Cord Injury and Improves Neurological Function via the Extracellular-Regulated Protein Kinase Signaling Pathway. Mol Neurobiol 57 (10):3993-4006. doi:10.1007/s12035-020-01997-0
60. Dong XQ, Yu WH, Hu YY, Zhang ZY, Huang M (2011) Oxymatrine reduces neuronal cell apoptosis by inhibiting Toll-like receptor 4/nuclear factor kappa-B-dependent inflammatory responses in traumatic rat brain injury. Inflamm Res 60 (6):533-539. doi:10.1007/s00011-010-0300-7
61. Ge XH, Shao L, Zhu GJ (2018) Oxymatrine attenuates brain hypoxic-ischemic injury from apoptosis and oxidative stress: role of p-Akt/GSK3beta/HO-1/Nrf-2 signaling pathway. Metab Brain Dis 33 (6):1869-1875. doi:10.1007/s11011-018-0293-4
62. Li W, Yao S, Li H, Meng Z, Sun X (2021) Curcumin promotes functional recovery and inhibits neuronal apoptosis after spinal cord injury through the modulation of autophagy. J Spinal Cord Med 44 (1):37-45. doi:10.1080/10790268.2019.1616147
63. Liu D, Huang Y, Jia C, Li Y, Liang F, Fu Q (2015) Administration of antagomir-223 inhibits apoptosis, promotes angiogenesis and functional recovery in rats with spinal cord injury. Cell Mol Neurobiol 35 (4):483-491. doi:10.1007/s10571-014-0142-x
64. Tsujimoto Y (2002) Bcl-2 family of proteins: life-or-death switch in mitochondria. Biosci Rep 22 (1):47-58. doi:10.1023/a:1016061006256
65. Xing S, Zhang Y, Li J, Zhang J, Li Y, Dang C, Li C, Fan Y, Yu J, Pei Z, Zeng J (2012) Beclin 1 knockdown inhibits autophagic activation and prevents the secondary neurodegenerative damage in the ipsilateral thalamus following focal cerebral infarction. Autophagy 8 (1):63-76. doi:10.4161/auto.8.1.18217
66. Luo CL, Li BX, Li QQ, Chen XP, Sun YX, Bao HJ, Dai DK, Shen YW, Xu HF, Ni H, Wan L, Qin ZH, Tao LY, Zhao ZQ (2011) Autophagy is involved in traumatic brain injury-induced cell death and contributes to functional outcome deficits in mice. Neuroscience 184:54-63. doi:10.1016/j.neuroscience.2011.03.021
67. Hao HH, Wang L, Guo ZJ, Bai L, Zhang RP, Shuang WB, Jia YJ, Wang J, Li XY, Liu Q (2013) Valproic acid reduces autophagy and promotes functional recovery after spinal cord injury in rats. Neurosci Bull 29 (4):484-492. doi:10.1007/s12264-013-1355-6
68. Ding K, Xu J, Wang H, Zhang L, Wu Y, Li T (2015) Melatonin protects the brain from apoptosis by enhancement of autophagy after traumatic brain injury in mice. Neurochem Int 91:46-54. doi:10.1016/j.neuint.2015.10.008
69. Zhang YB, Li SX, Chen XP, Yang L, Zhang YG, Liu R, Tao LY (2008) Autophagy is activated and might protect neurons from degeneration after traumatic brain injury. Neurosci Bull 24 (3):143-149. doi:10.1007/s12264-008-1108-0
70. Li Z, Chen T, Cao Y, Jiang X, Lin H, Zhang J, Chen Z (2019) Pros and Cons: Autophagy in Acute Spinal Cord Injury. Neurosci Bull 35 (5):941-945. doi:10.1007/s12264-019-00368-7

71. Tanabe F, Yone K, Kawabata N, Sakakima H, Matsuda F, Ishidou Y, Maeda S, Abematsu M, Komiya S, Setoguchi T (2011) Accumulation of p62 in degenerated spinal cord under chronic mechanical compression: functional analysis of p62 and autophagy in hypoxic neuronal cells. Autophagy 7 (12):1462-1471. doi:10.4161/auto.7.12.17892
72. Bai L, Mei X, Shen Z, Bi Y, Yuan Y, Guo Z, Wang H, Zhao H, Zhou Z, Wang C, Zhu K, Li G, Lv G (2017) Netrin-1 Improves Functional Recovery through Autophagy Regulation by Activating the AMPK/mTOR Signaling Pathway in Rats with Spinal Cord Injury. Sci Rep 7:42288. doi:10.1038/srep42288

Figures

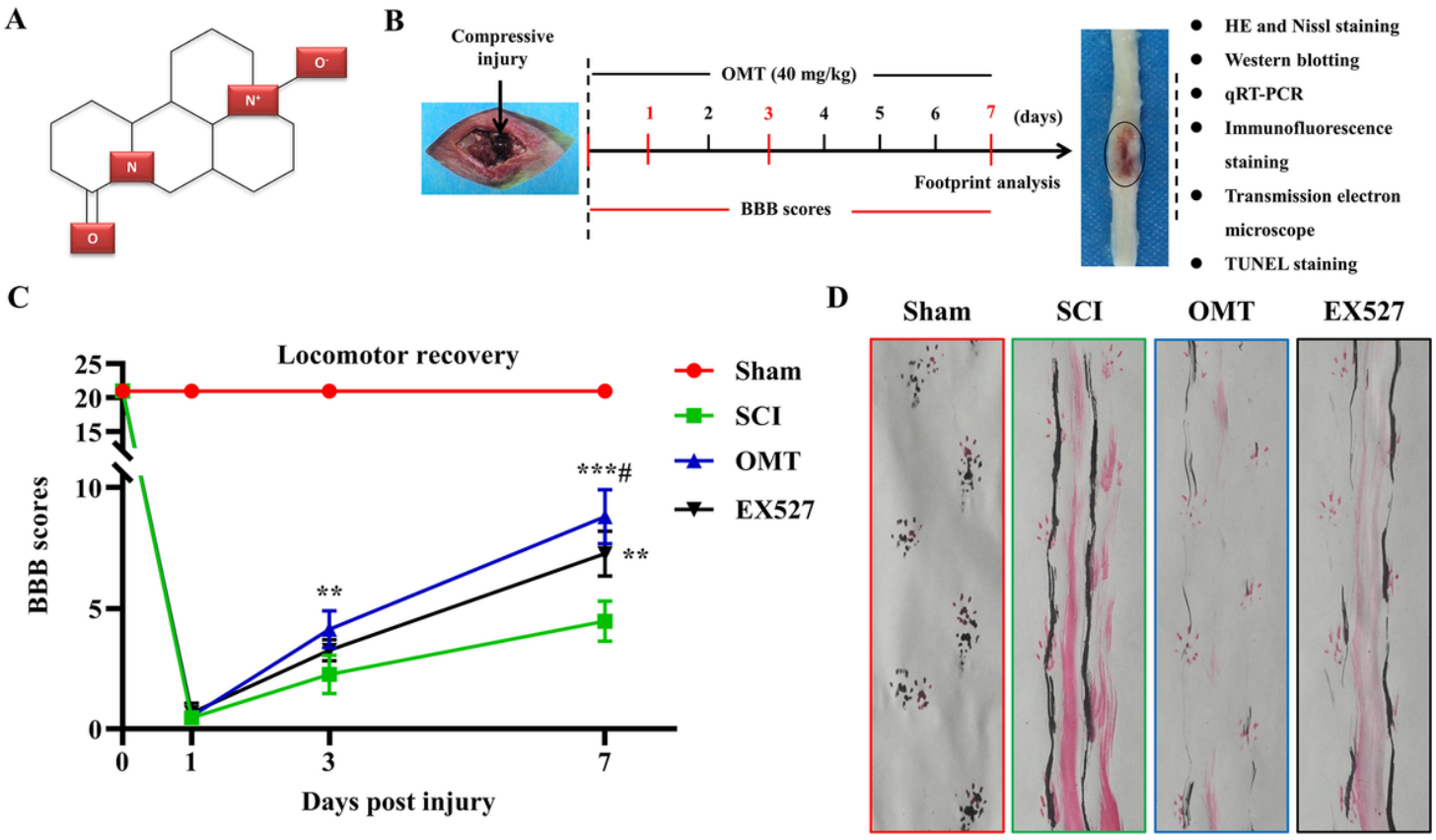

Figure 1

Effects of OMT treatment on locomotor functions after SCI in rats. (A) Chemical structure of oxymatrine. (B) The schematic diagram of experimental procedures. (C) BBB scores in animals of the different treatment groups at days 0, 1, 3, and 7 post SCI (n=5). Obviously, compared with the SCI group, The BBB scores were significantly higher in the OMT-treated group at day 3 and at day 7, and in the OMT-EX527 co-treatment group at day 7. Data are presented as mean ± SEM, significant differences among groups are indicated by $^{\#}P < 0.05$, $^{**}P < 0.01$, and $^{***}P < 0.001$. (D) Footprint analysis in animals of the different treatment groups. Apparently, rats treated with OMT showed clear hindlimb coordination and little toe

dragging compared with the SCI rats. Red indicates forepaw footprints; Black indicates hindpaw footprints.

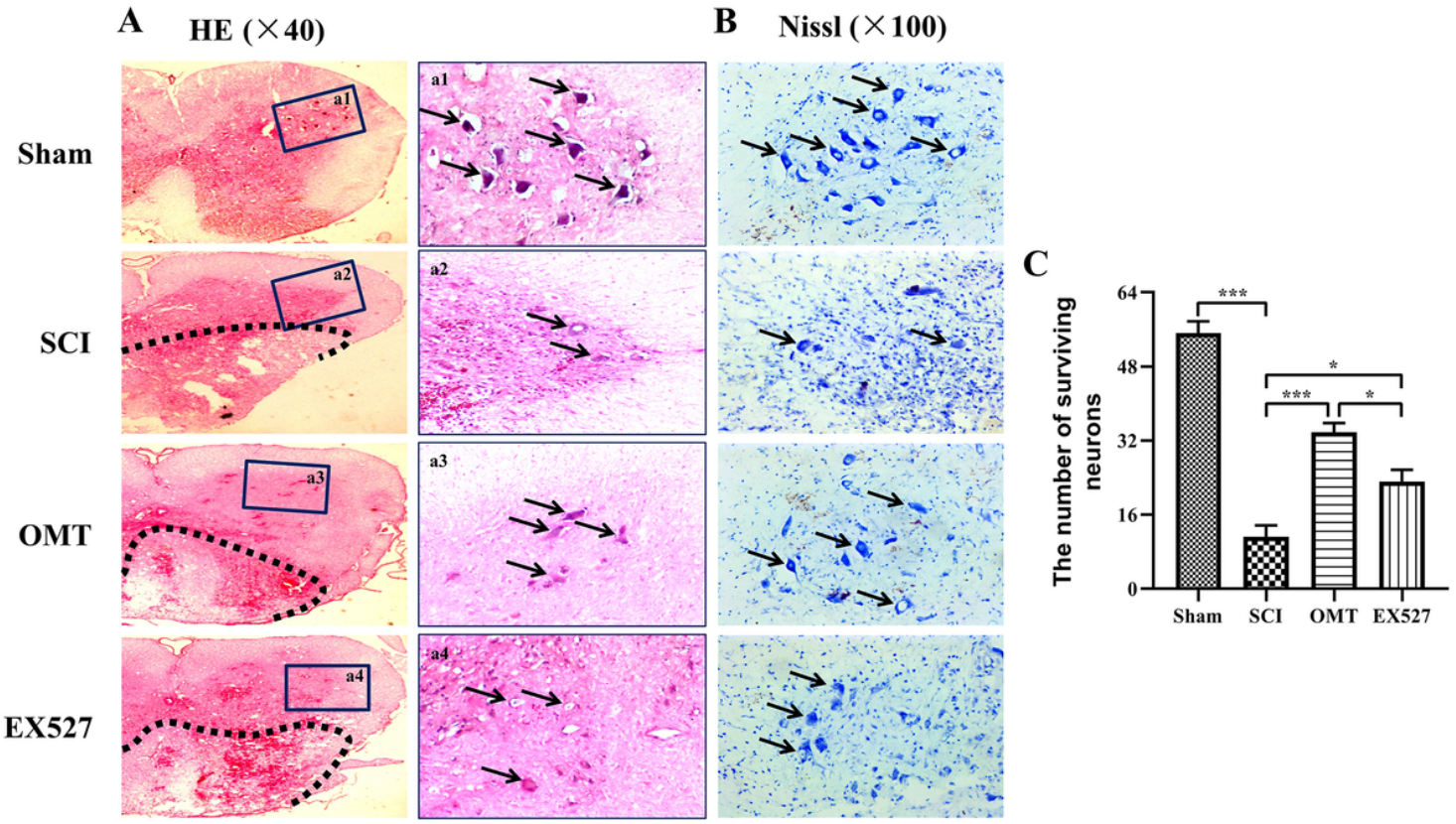

Figure 2

Effects of OMT treatment on neural tissue damage and neuronal survival after SCI in rats at day 7. (A) Representative HE staining images of the spinal cord in animals of the different treatment groups after SCI. Black dotted lines in the images indicate the border of the cavity area and black arrows indicate surviving neurons. Rats treated with OMT or OMT and EX527 showed a significantly reduced lesion in the injured spinal cord. Scale bars = 400 μm. (B-C) Representative Nissl staining images and quantitative analysis of ventral horn motor neurons surrounding the lesion epicenter in the different treatment groups after SCI (n=5). Black arrows indicate the surviving neurons. Rats treated with OMT or OMT and EX527 showed significantly increased numbers of surviving neurons compared to untreated animals with SCI, but the number of surviving neurons was significantly decreased in the OMT-EX527 co-treatment group compared with the OMT-only group. Scale bars = 50 μm. Data are presented mean ± SEM, significant differences among groups are indicated by $^{*}P<0.05$ and $^{***}P<0.001$.

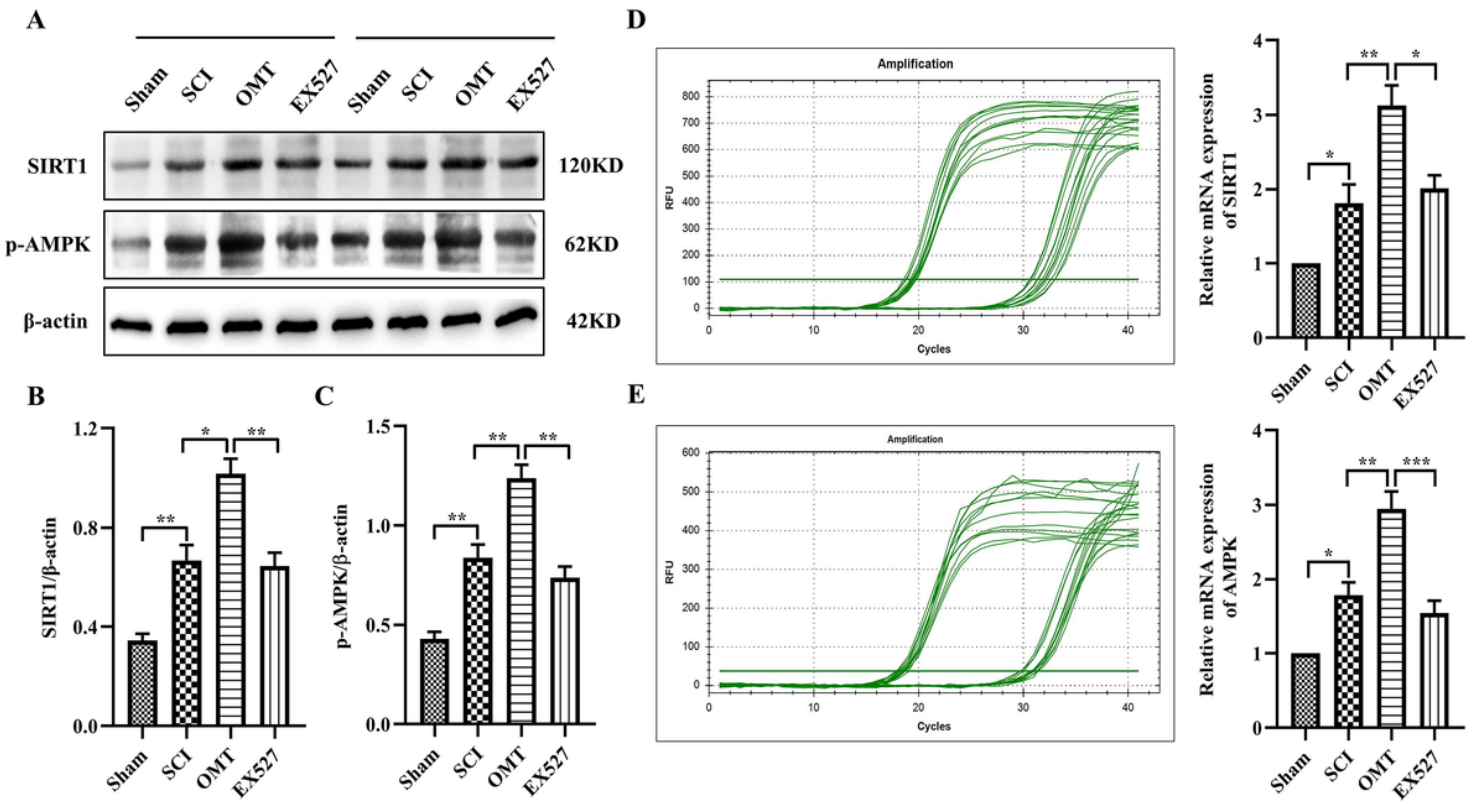

Figure 3

Effect of OMT treatment on SIRT1 and AMPK protein expression after SCI in rats at day 7. (A-C) Representative Western blotting and quantitative results of SIRT1 and p-AMPK after SCI (n=6). Rats treated with OMT or OMT and EX527 exhibited a significantly increased expression of SIRT1 and p-AMPK after injury, while the levels of SIRT1 and p-AMPK expression were significantly decreased in the OMT-EX527 co-treatment group compared with the OMT-only group. (D-E) qRT-PCR and quantitative analysis of SIRT1 and AMPK mRNAs expression after SCI (n=8). Rats treated OMT or OMT and EX527 had a significantly higher expression of SIRT1 and AMPK mRNAs following SCI compared to untreated animals but the levels of both genes were significantly reduced in the OMT-EX527 co-treated group compared with the OMT-only group. Data are presented mean ± SEM, significant differences among groups are indicated by $^{*}P<0.05$, $^{**}P<0.01$, and $^{***}P<0.001$.

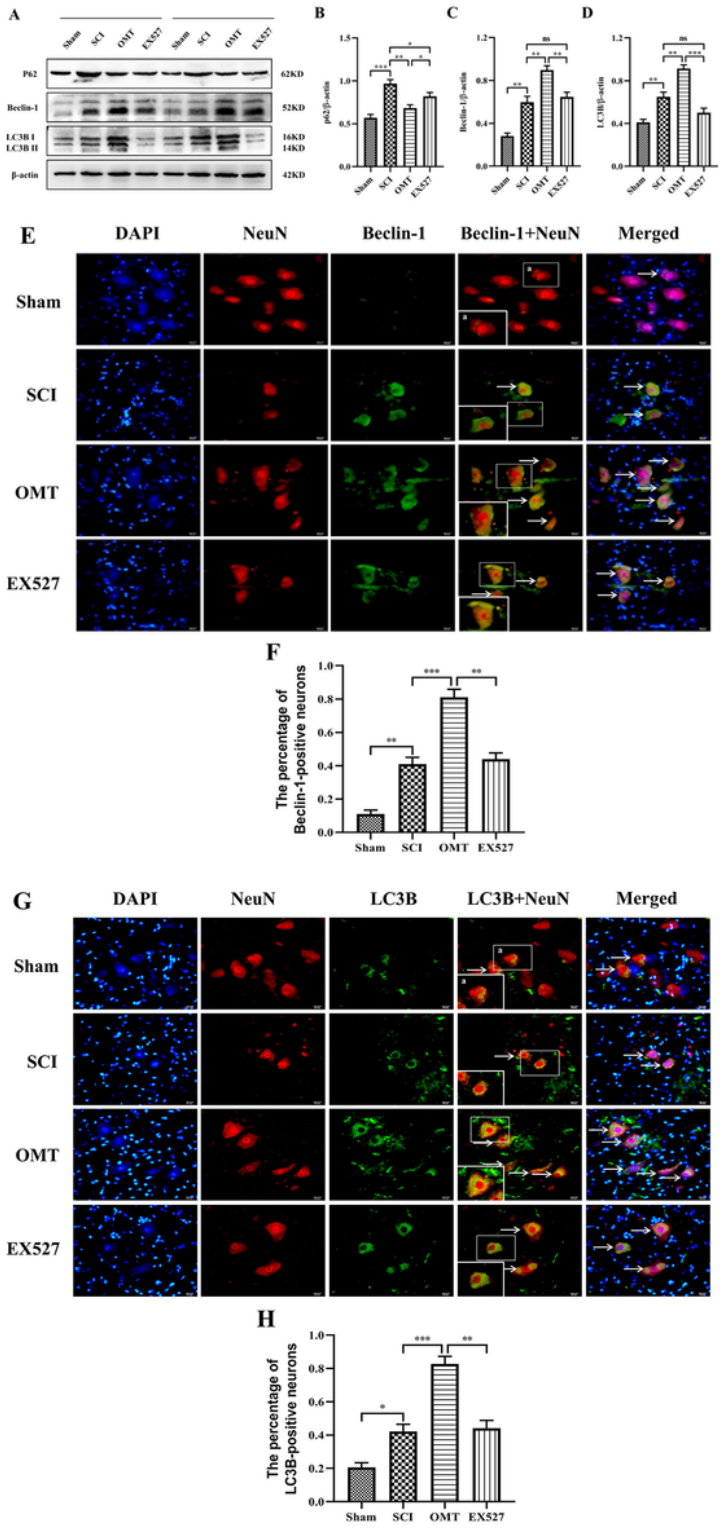

Figure 4

Effect of OMT treatment on neuronal autophagy after SCI in rats at day 7. (A-D) Representative Western blotting and quantitative results of p62, Beclin-1 and LC3B after SCI (n=6). Rats treated with OMT or OMT and EX527 showed a significantly increased expression of Beclin-1 and LC3B but decreased expression of p62 after injury, while the levels of Beclin-1 and LC3B expression were significantly decreased with concomitant upregulation of autophagy substrate protein p62 in the OMT-EX527 co-treatment group

compared with the OMT-only group. (E-H) Representative immunofluorescence double staining images of Beclin-1(green)/Neuron(red) and LC3B(green)/Neuron(red), as well as the quantitative analysis of Beclin-1 and LC3B in the ventral horns of spinal cord after SCI (n=5). White arrows point to the co-localization of Beclin-1 or LC3B with neurons. Rats treated OMT or OMT and EX527 showed a significantly increased number of Beclin-1 or LC3B-positive neurons after injury, the number of Beclin-1 or LC3B-positive neurons was significantly lower in the OMT-EX527 co-treated group compared with the OMT-only group. Scale bar = 20 μm. Data are presented as mean ± SEM, significant differences among groups are indicated by $^{*}P<0.05$, $^{**}P<0.01$, and $^{***}P<0.001$.

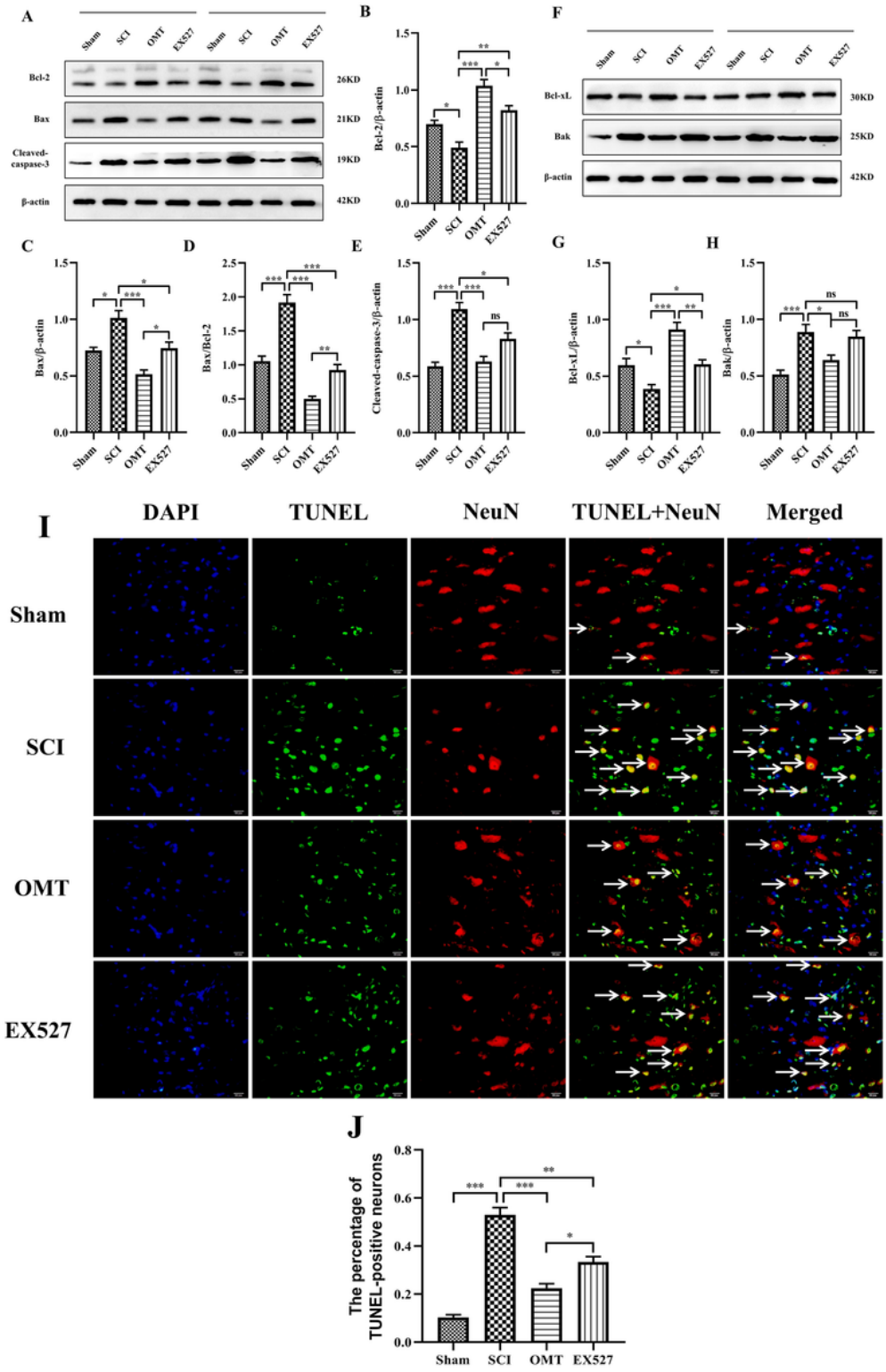

Figure 5

Effect of OMT treatment on neuronal apoptosis after SCI in rats at day 7. (A-H) Representative Western blotting and quantitative results of Bcl-2, Bcl-xL, Bax, C-caspase-3 and Bak after SCI (n=6). Rats treated OMT or OMT and EX527 exhibited a significantly decreased expression of Bax, C-caspase-3 and Bak, as well as the ratio of Bax/Bcl-2 and significantly increased expression of Bcl-2 and Bcl-xL proteins after injury compared to the untreated animals. After co-treatment with OMT and EX527, the levels of Bax

expression and the ratio of Bax/Bcl-2 were significantly increased and Bcl-2 and Bcl-xL levels were significantly reduced compared with the OMT-only group. (I-J) Representative immunofluorescence double staining images of TUNEL(green)/Neuron(red), as well as the quantitative analysis of TUNEL-positive neurons after SCI (n=5). White arrows point to the representative TUNEL-positive neurons. Rats treated OMT or OMT and EX527 showed a significantly decreased number of TUNEL-positive neurons. The number of TUNEL-positive neurons was significantly increased in the OMT-EX527 co-treated group compared with the OMT-only group. Scale bar is 20 μm. Data are presented mean ± SEM, significant differences among groups are indicated by $^{*}P<0.05$, $^{**}P<0.01$, and $^{***}P<0.001$.

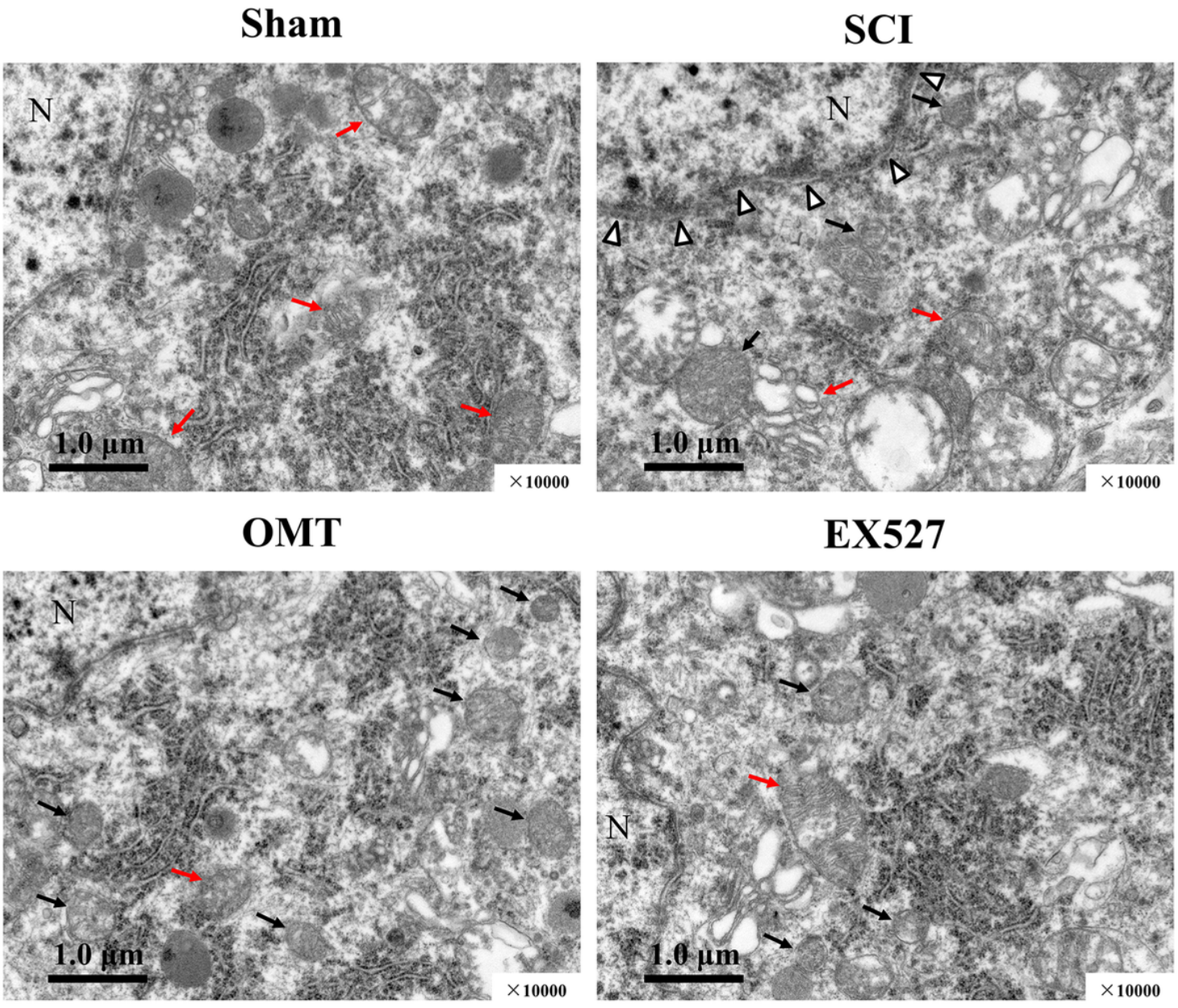

Figure 6

Effect of OMT treatment on neuronal ultrastructures after SCI in rats at day 7. Representative electron micrographs of spinal cord neurons in animals of the different treatment groups after SCI. In the sham-

group rats, neurons demonstrated barely autophagosomes, but displayed clear nuclear structure and intact mitochondria with clearly visible crista. In contrary, in the SCI-group rats, neurons were seriously damaged and exhibited abnormal intracellular structures including chromatin condensation and karyotin margination, mitochondria swelling and cytoplasm vacuolation, as well as numerous double-membrane structure autophagosomes. However, rats treated with OMT or OMT and EX527 significantly alleviated these morphological impairments of ventral neurons of spinal cord and enhanced the number of autophagosomes. Scale bar = 1 μm. (N, nucleus; the dovetail arrows indicate karyotin margination; the red arrow points to mitochondria; the black arrow identifies an autophagosome).

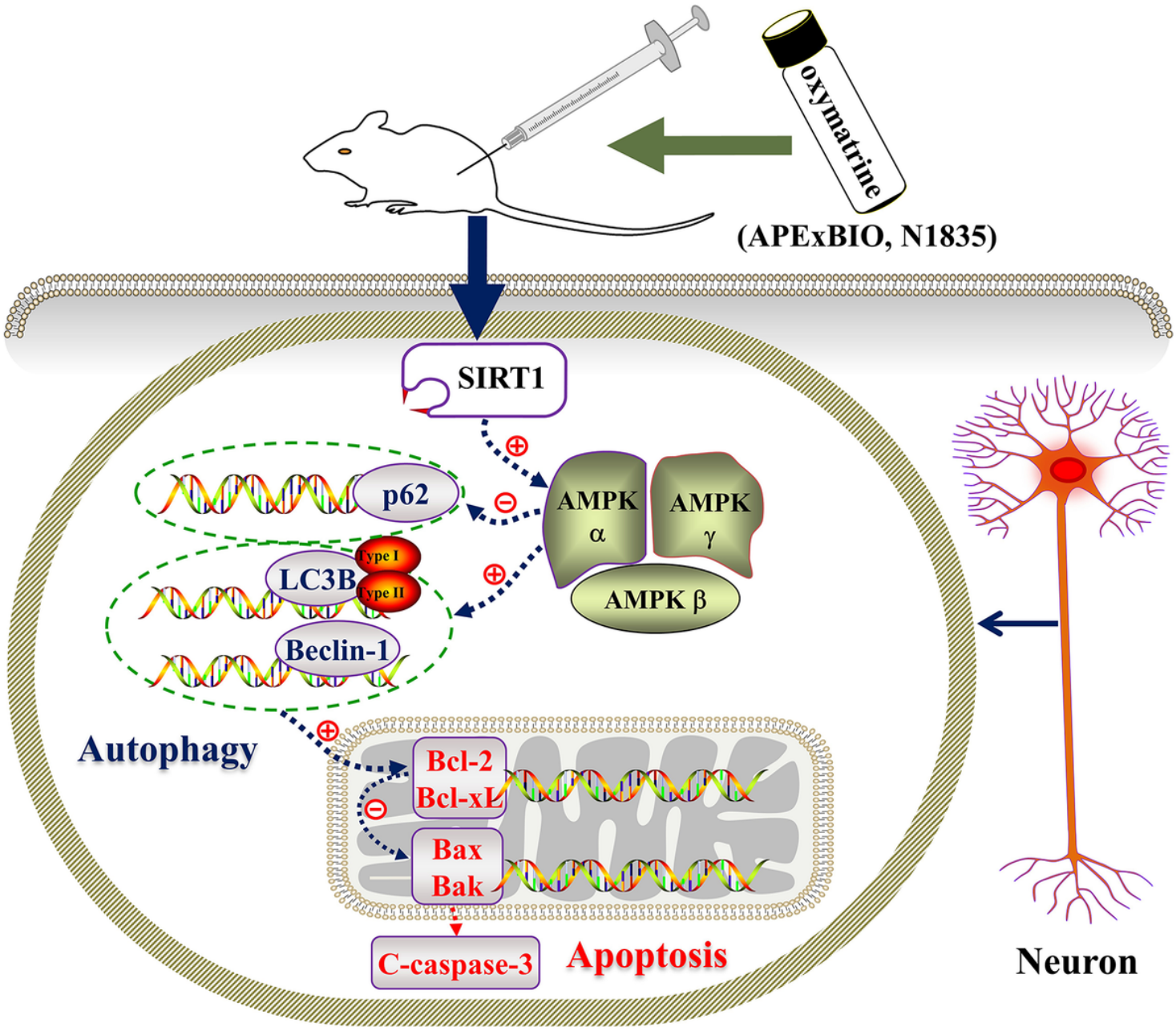

Figure 7

Schematics of a proposed mechanism underlying the neuroprotective effect of OMT against SCI. OMT promotes SCI-induced neuronal autophagy, inhibits neuronal apoptosis via activation of the SIRT1/AMPK

signaling pathway in a SCI rat model.